Bulk and surface electronic structures of Si(111)2×1 and Si(111)7×7 studied by angle-resolved photoelectron spectroscopy

R. I. G. Uhrberg, G. V. Hansson, U. O. Karlsson, J. M. Nicholls, and P. E. S. Persson
Department of Physics and Measurement Technology, Linköping University, S-581 83 Linköping, Sweden

S. A. Flodström
MAX-LAB, Box 725, S-220 07 Lund, Sweden

R. Engelhardt
II. Institut für Experimentalphysik der Universität Hamburg, D-2000 Hamburg 50, Germany

E.-E. Koch
Hamburger Synchrotronstrahlungslabor (HASYLAB), Deutsches Elektronen-Synchrotron (DESY), D-2000 Hamburg 52, Germany

(Received 1 June 1984)

By using polarization-dependent angle-resolved photoemission bulk direct transitions from the uppermost two valence bands have been identified in spectra for both Si(111)2×1 and Si(111)7×7. The experimental initial-energy versus $\bar{k}_{\parallel}$ dispersions for these transitions obtained in the $(1\bar{1}0)$ mirror plane, are in good agreement with calculated dispersions for transitions to a free-electron final band in the photon-energy range 10.2—17.0 eV investigated. The surface electronic structure of cleaved Si(111)2×1 is compared with that of the Si(111)7×7 surface obtained both by annealing a cleaved sample and by sputtering and annealing a polished sample. The two ways of preparing the 7×7 surface result in essentially identical surface electronic structures.

I. INTRODUCTION

Angle-resolved photoemission spectroscopy has been shown by several authors to be a very powerful technique for obtaining information about the electronic band structure of different materials.[1,2] Experimental energy-band structures have been obtained for several metals, but only for a few semiconductors. GaAs is an often cited example, for which the valence bands have been mapped along several high symmetry lines in the Brillouin zone.[3] More recently this technique was applied to Ge(100) for which valence-band dispersions along the $\Gamma-X$ line were obtained in a normal emission experiment.[4] In spite of extensive studies of different Si surfaces, no detailed information about its bulk band structure has hitherto been presented. The general approach in band mapping is to assume a free-electron final state for the photoemission process. Since the conduction-band structure of semiconductors is very complicated, it is difficult to find a final-state band, sufficiently free-electron-like in character to motivate the use of a free-electron final-state band. This is particularly the case when low photon energies are used.

In this paper we report polarization-dependent angle-resolved photoemission measurements from Si(111)2×1. From normal emission data, in the photon energy range 10.2—21.2 eV, we have found an experimental final-state band with a free-electron-like dispersion. Using this band, we can identify direct transitions from the uppermost two valence bands. $E_i(\bar{k}_{\parallel})$ dispersion relations for these transitions were obtained from off-normal emission in the photon-energy range 10.2—17.0 eV. These are found to be in good agreement with calculated dispersions. A similar comparison between experimental and calculated $E_i(\bar{k}_{\parallel})$ dispersions have been reported for Ge(111) by Bringans and Höchst,[5] who also identified direct transitions from the two uppermost valence bands.

The direct transitions from the uppermost valence band for Si(111)2×1 give rise to a prominent peak in the spectra at 10.2-eV photon energy in the $[11\bar{2}]$ azimuthal direction. This structure was first reported by Rowe *et al.*[6] and has so far been interpreted in the literature as a surface state. Our interpretation of this structure as being due to bulk transitions explains in a natural way the threefold emission pattern observed.

We also report on measurements performed using unpolarized light in which the bulk and surface electronic structures of Si(111)2×1 and Si(111)7×7 are compared. The transitions from the uppermost valence band are also observed for Si(111)7×7, while the surface-state emission looks entirely different from that of Si(111)2×1.

II. EXPERIMENTAL DETAILS

Angle-resolved photoemission spectra were recorded using two different experimental setups. In the first study, photoemission data from Si(111)2×1 in the $[11\bar{2}]$-azimuthal direction were obtained in a VG ADES 400 spectrometer using synchrotron radiation from the DORIS II storage ring at HASYLAB, DESY.[7] The electron analyzer was rotatable in both the horizontal and vertical planes. Two different geometries were used in these measurements.

(1) The light was incident normally ($\theta_i = 0°$) with its polarization vector lying in the $(1\bar{1}0)$ mirror plane, parallel to the $[11\bar{2}]$ direction. For emission angles (θ_e) between 0° and 10°, $\theta_i = 15°$ was used. This geometry will be referred to as the $\bar{A}_{\parallel}$ case.

(2) Both the analyzer plane and the crystal were rotated 90° azimuthally as compared to geometry (1). Because of experimental limitations, $\theta_i = 15°$ was selected instead of $\theta_i = 0°$. This makes the direction of light polarization essentially perpendicular to the mirror plane. This geometry will be referred to as the $\bar{A}_{\perp}$ case. The total-energy resolution was $\lesssim 0.2$ eV at a photon energy of 10.2 eV and $\lesssim 0.25$ eV at 13.0 eV.

In the second study, photoemission spectra from Si(111)2×1 and Si(111)7×7 were obtained in both the $[11\bar{2}]$- and $[\bar{1}\bar{1}2]$-azimuthal directions using monochromatized light from a hydrogen discharge. The electrons emitted were analyzed by a 180° spherical deflection analyzer. The total-energy resolution in the recorded spectra was $\lesssim 0.2$ eV at the photon energy of 10.2 eV.

The initial energies have been referenced to the valence-band maximum (VBM) for Si(111)2×1 by comparing the energy of the bulk structure A for 10.2-eV photon energy in Fig. 1 with that for Si(111)7×7. For Si(111)7×7, we have used $E_F - E_V = 0.59$ eV.[8] The Fermi-level (E_F) reference was determined to an accuracy of ±0.05 eV by photoelectron emission from the sample holder. LEED was used in both experimental setups to characterize the surface reconstruction.

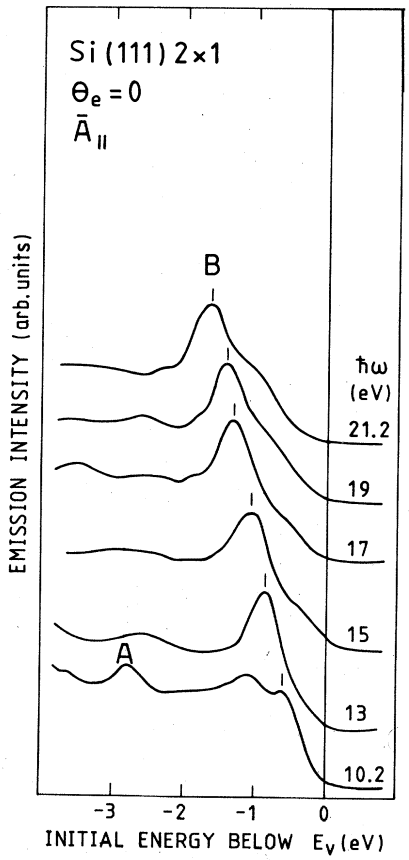

FIG. 1. Normal emission spectra from Si(111)2×1 for various photon energies. Structure A was used to determine the valence-band maximum. Structure B corresponds to direct transitions in the bulk.

III. EXPERIMENTAL RESULTS

A. Si(111)2×1: Normal emission and $[1\bar{1}2]$ azimuth

The 2×1 reconstructed surfaces were obtained by cleaving Si(111) single crystals, of p type ($\rho \sim 43\ \Omega$ cm), inside the UHV chamber at a pressure of $\sim 1\times10^{-10}$ Torr. Normal-emission spectra in the photon-energy range 10.2—21.2 eV for the $\bar{A}_{\parallel}$ case shown in Fig. 1 exhibit one dominating structure, denoted B. This structure disperses downwards with increasing photon energy, having initial energies from −0.60 to −1.60 eV. The variation of initial energy with photon energy suggests interpreting this structure as a direct transition.

Bulk energy bands for Si, obtained from a self-consistent-field linearized augmented-plane-wave (LAPW) (Ref. 9) calculation, are shown in Fig. 2 along the Γ—L and Γ—K symmetry lines. Using the calculated bands

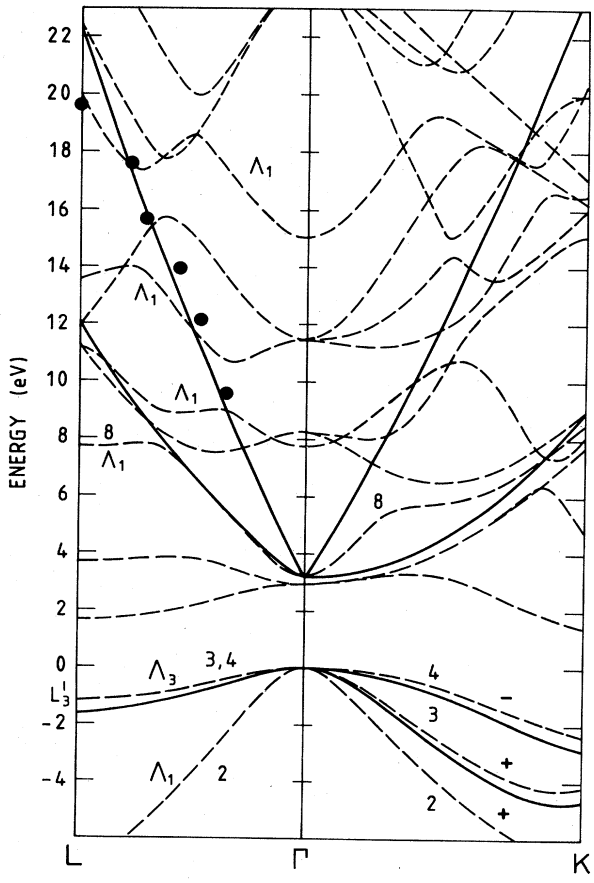

FIG. 2. Calculated band structure for silicon along the Γ—L and Γ—K symmetry lines (dashed lines). The experimental final band for structure B (solid circles) was obtained using the experimental valence band (solid line). The final band is approximated by the $\bar{k} + \bar{G}_{111}$ free-electron band. Included are also the degenerate $\bar{k} + \bar{G}_{\bar{1}11}$ and $\bar{k} + \bar{G}_{1\bar{1}1}$ free-electron bands.

along the $\Gamma-L$ line, we can try to identify the initial and final bands involved in a direct transition giving rise to structure B. There are three valence bands in the region of experimental initial energies. The $\bar{k}$ points along the $\Gamma-L$ line at which the direct transitions take place are determined by the initial energies from Fig. 1, and by adding the corresponding photon energy, the experimental final band is obtained. The application of this procedure to valence band (VB) 2 results in a very steep experimental final band, incompatible with any calculated conduction bands or assumed free-electron final bands. This lets us exclude VB 2 as a possible initial band in this case.

The degenerate VB's 3,4 would give a final band with a realistic dispersion, but still they cannot account for all the experimental initial energies, since the calculated L_3' point is too high in energy. The calculated L_3' point energy is -1.15 eV, in good agreement with other calculations,[10] while the lowest experimental initial energy is -1.60 eV. In a recent photoemission experiment, Himpsel *et al.*[11] found the L_3' point (reported to be probed in normal emission at a photon energy of 21 eV) at -1.5 eV. Accordingly, we find the L_3'-point energy to be -1.6 eV from the 21.2-eV spectrum, in close agreement with the earlier experiment. In Fig. 2 we have introduced an experimental valence band (solid line) which is lowered with respect to the calculated band. The lowering is proportional to the distance from Γ so that the L_3'-point energy becomes -1.60 eV. The final band obtained by using this experimental initial band is plotted as solid circles in Fig. 2. For some energies, 21.2. 19.0, and 13.0 eV, the final-state points are close to calculated final bands of Λ_1 symmetry, which is the proper symmetry for normal emission, while for 15.0 eV and especially for 17.0 eV we find a large deviation from calculated Λ_1-final bands. At the photon energy of 17.0 eV the final state lies in the middle of the Λ_1 hybridization gap, ~ 1.7 eV from the nearest Λ_1 band. We did not observe any decrease in the emission intensity of structure B, for excitation to the hybridization gap region. Taking all photon energies into account, one finds that the experimental final band is better described by a free-electron-like band than by the calculated final bands. This finding will be used in the analysis below.

The initial-energy dispersion as a function of the electron wave vector parallel to the surface, $E_i(\bar{k}_{||})$, has been measured for structure B at four different photon energies (10.2, 13.0, 15.0, and 17.0 eV). A comparison between experimental and calculated $E_i(\bar{k}_{||})$ dispersions is one way of discriminating among different initial- and final-band assignments for structure B. Using calculated final bands, such a comparison has turned out to be very complicated. In general, one obtains different dispersion branches which lie in the same $E_i-\bar{k}_{||}$ region, originating from transitions to different final bands. To be able to distinguish among the different branches, one would have to calculate the transition matrix elements and compare them with experimental intensities. The overall shapes and energy positions of the experimental $E_i(\bar{k}_{||})$ dispersions are also difficult to reproduce using calculated final bands. This is particularly obvious at a photon energy of 17.0 eV for which the experimental final state lies in the Λ_1 gap far from the calculated bands. Furthermore, a rather large uncertainty is introduced in the comparison since the calculated final bands could be off by as much as ~ 1 eV at the higher final energies.

We will instead proceed by taking advantage of the experimentally obtained free-electron-like final band. To be able to calculate the $E_i(\bar{k}_{||})$ dispersions using this final band, we have approximated it by the $\bar{k}+\bar{G}_{111}$ free-electron band (see Fig. 2). This "primary cone" band has been fitted in energy to the experimental points for normal emission. This places the bottom of the free-electron bands at -12.1 eV. We have also assumed the lowering of VB's 3 and 4, described above, in the whole mirror plane.

We will now compare experimental and calculated $E_i(\bar{k}_{||})$ dispersions for direct transitions from VB's 3 and 4 to the free-electron final band at photon energies of 10.2, 13.0, 15.0, and 17.0 eV. Angle-resolved photoemission spectra were obtained for both the $\bar{A}_{||}$ and $\bar{A}_{\perp}$ cases. The different polarization conditions are used to determine the initial-state parity with respect to the mirror plane.[12] The initial energies of structure B for various emission angles (θ_e) are shown in Fig. 3 for a photon energy of 10.2 eV. Structure B first disperses downwards to a local minimum in initial energy at $\theta_e \sim 20°$, then upwards to a local maximum at $\theta_e \sim 40°$, and finally moves downwards again at higher emission angles. The $E_i(\bar{k}_{||})$ dispersion obtained from these spectra is plotted as solid and open squares in Fig. 5. For the $\bar{A}_{||}$ case the initial state should have even parity, which corresponds to VB 3. The calculated $E_i(\bar{k}_{||})$ dispersion using this initial band is shown by the dashed-dotted line in Fig. 5. The calculated dispersion is in good agreement with the experimental one, with regard to both energy position and the overall shape.

As shown in Fig. 4 the spectra obtained for the $\bar{A}_{\perp}$ case are very different from the $\bar{A}_{||}$ spectra. There is a dominating structure, denoted C, with maximum intensity around $\theta_e = 20°$ not observed for the $\bar{A}_{||}$ case. The $E_i(\bar{k}_{||})$ dispersion of this structure is plotted as solid and open circles in Fig. 5. The dashed curve shows the calculated dispersion using VB 4 which has the appropriate odd parity. For this structure C we again find good agreement between experimental and calculated dispersions. The energy positions of structures B and C will coincide for transitions on the $\Gamma-L$ line in the $[11\bar{1}]$ direction. This occurs for both the experimental and the calculated dispersions at $\bar{k}_{||} \sim 0.7$ Å^{-1}, as can be seen in Fig. 5.

Structures B and C were also observed at 13.0, 15.0, and 17.0 eV and had qualitatively similar $E_i(\bar{k}_{||})$ dispersions. Spectra obtained at 13.0 eV for the $\bar{A}_{||}$ case are shown in Fig. 6. Close to normal emission we find structure B having high emission intensity, which has decreased drastically in the $\theta_e = 10°$ spectrum. For higher emission angles $\theta_e \geq 20°$, there is a structure dispersing first upwards in initial energy to a maximum around 45° and then downwards, in qualitative agreement with what was found for structure B at 10.2-eV photon energy. Turning to the $\bar{A}_{\perp}$ case (Fig. 7) we can positively identify structure C for $\theta_e \geq 15°$. The experimental $E_i(\bar{k}_{||})$ dispersions for structures B and C are plotted in Fig. 8 together

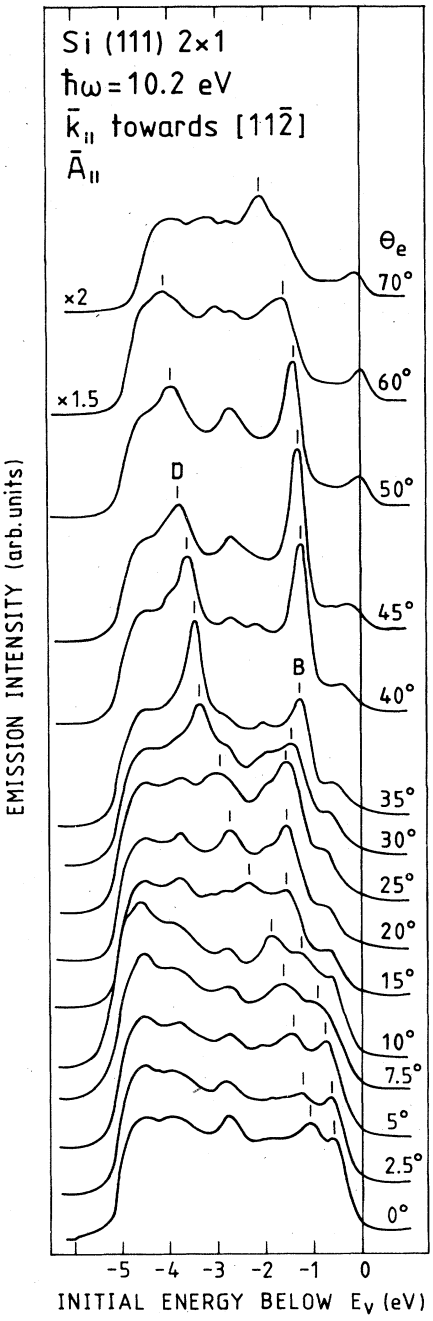

FIG. 3. Photoemission spectra for different angles for the $\bar{A}_{\parallel}$ case. Structure *B* corresponds to direct transitions from the second-highest, even-parity, valence band. Structure *D* is also interpreted as a direct transition; see text for details.

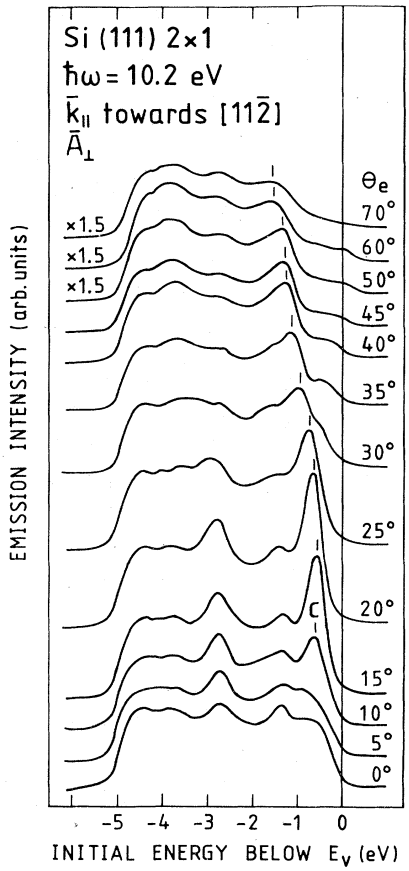

FIG. 4. Photoemission spectra for different angles for the $\bar{A}_{\perp}$ case. Structure *C* corresponds to direct transitions from the uppermost, odd-parity, valence band.

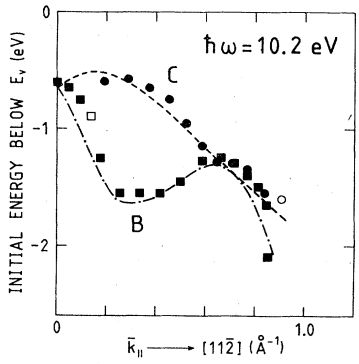

FIG. 5. Experimental $E_i(\bar{k}_{\parallel})$ dispersions for structure *C* (solid and open circles corresponding to strong and weak structures) and structure *B* (solid and open squares). The calculated dispersions for direct transitions from the odd- and even-parity valence bands (dashed and dashed-dotted lines) are in close agreement with experimental dispersions.

with calculated dispersions using VB's 3 and 4, respectively. Open circles near $\bar{k}_{\parallel}=0$ indicate the uncertainty in the assignment of the structure. Similar experimental and calculated dispersions shown in Fig. 9 were also obtained for 15.0- and 17.0-eV photon energy. As can be seen from Figs. 8 and 9, we also find good agreement between exper-

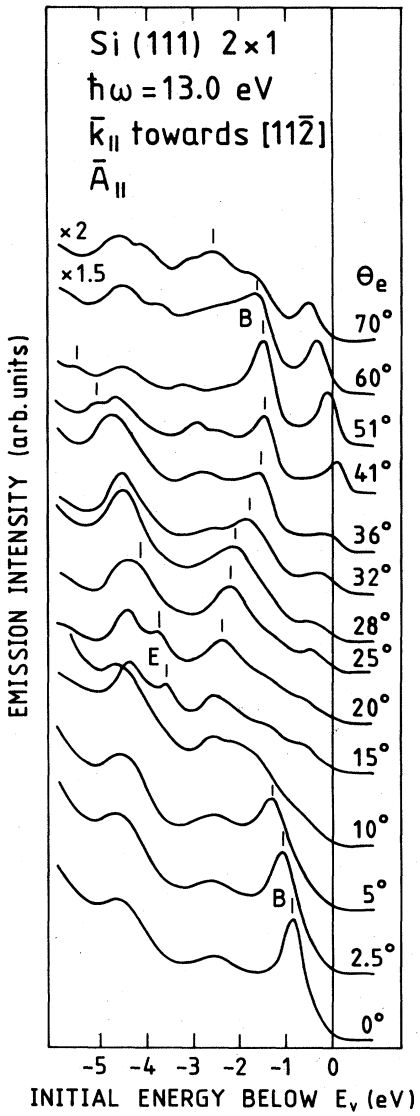

FIG. 6. Photoemission spectra for different angles for the $\bar{A}_{\parallel}$ case. Structure B corresponds to direct transitions from the second-highest, even-parity, valence band. The origin of structure E is discussed in the text.

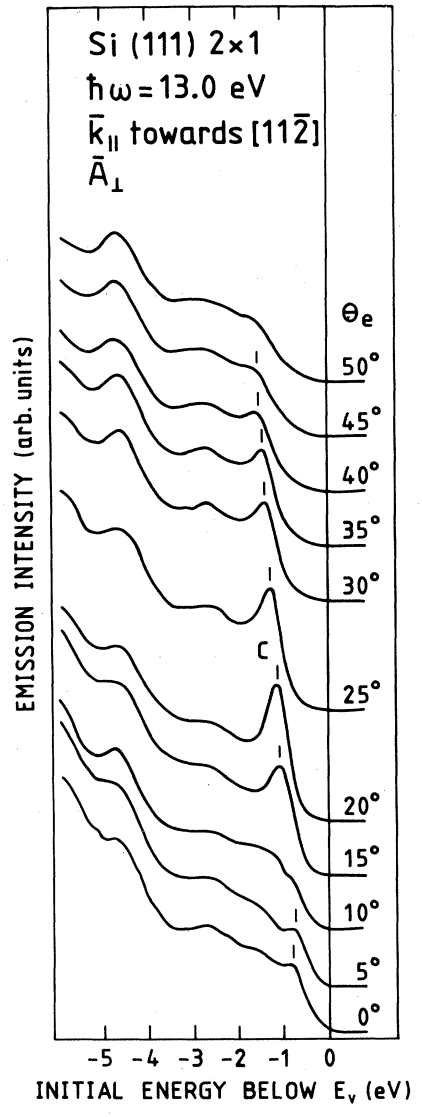

FIG. 7. Photoemission spectra for different angles for the $\bar{A}_{\perp}$ case. Structure C corresponds to direct transitions from the uppermost, odd-parity, valence band.

imental and calculated $E_i(\bar{k}_{\parallel})$ dispersions for structures B and C at higher photon energies.

One virtue of the free-electron-like final band is that it gives different initial energies for transitions on the Γ—L line in the [111] direction, compared with transitions on the Γ—L line in the [11$\bar{1}$] direction, which is also observed experimentally for the different photon energies. Calculated final bands would instead have given the same initial energies for transitions on the Γ—L lines in the two different directions.

As discussed elsewhere,[13] structure C, first reported by Rowe *et al.*,[6] has so far been interpreted as emission from a surface state. This interpretation is definitely ruled out by the significant changes in $E_i(\bar{k}_{\parallel})$ dispersion as a function of photon energy found for the photon energies investigated. The polarization dependence and the good agreement with calculated dispersions make us interpret both structures B and C as direct transitions from VB's 3 and 4, respectively, to a free-electron-like final band. Our interpretation of structure C as being a bulk feature explains in a natural way the threefold emission pattern observed.[6] The sensitivity of structures B and C to contamination was found to be far less than that observed for the dangling-bond surface state.[14] Knowledge of the origin of structures B and C provides a basis for a more detailed photoemission study of the experimental final bands, investigating the differences and similarities with calculated conduction bands for Si.

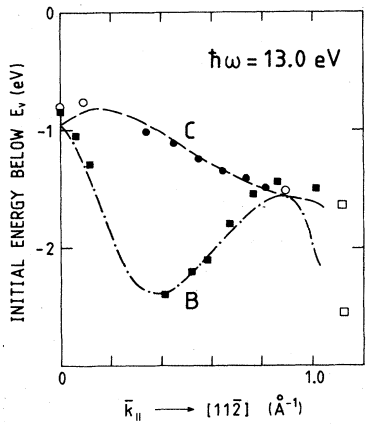

FIG. 8. Experimental and calculated $E_i(\bar{k}_{||})$ dispersions for structures B and C for $\hbar\omega = 13.0$ eV. For details see Fig. 5.

In the present experiment, where the [11$\bar{2}$] direction corresponds to the $\bar{\Gamma}$–$\bar{K}$ line in the 2×1 surface Brillouin zone, the dangling-bond surface state is observed as a weak structure dispersing towards the valence-band edge. Emission from the dangling bond is suppressed for both the $\bar{A}_{||}$ and $\bar{A}_{\perp}$ cases because of the angles θ_i used (0° and 15°, respectively). There also seems to be some effect of the different polarizations used on the emission intensity. The dangling-bond emission is weaker for the $\bar{A}_{\perp}$ case than for the $\bar{A}_{||}$ case at 10.2 eV, although the spectra were measured at approximately the same time after cleavage. In the $\bar{A}_{\perp}$ spectra obtained at 13.0 eV, the dangling-bond emission was further reduced by contamination since a longer time had elapsed after cleavage.

In the spectra obtained for the $\bar{A}_{||}$ case at 10.2 eV, we find another dispersive structure, denoted D, in Fig. 3. This structure disperses from -1.1 eV in normal emission down to -4 eV at $\theta_e = 60°$, having maximum intensity at $\theta_e = 35°$. We will discuss the origin of this structure as a direct transition both using free-electron and calculated final bands. In the case of free-electron final bands, we must also take the degenerate $\bar{k}+\bar{G}_{\bar{1}\bar{1}1}$ and $\bar{k}+\bar{G}_{\bar{1}11}$ free-electron bands into account. These free-electron bands are included in Fig. 2. There are two cases involving free-electron bands which could possibly account for the experimental $E_i(\bar{k}_{||})$ dispersion of structure D, plotted as solid circles in Fig. 10. Transitions from the lowered VB 3 to the $\bar{k}+\bar{G}_{\bar{1}\bar{1}1,\bar{1}11}$-type free-electron bands give the dispersion shown by the dashed line in Fig. 10. Transitions from the VB 2 to the $\bar{G}_{111}$ final band give the dispersion shown by the dashed-dotted line in Fig. 10. As seen from the figure, the calculated dispersions come close to each other for $\bar{k} \geq 0.15$ Å^{-1}, and within this region the intensity has its maximum at $\bar{k}_{||} \sim 0.4$ Å^{-1}.

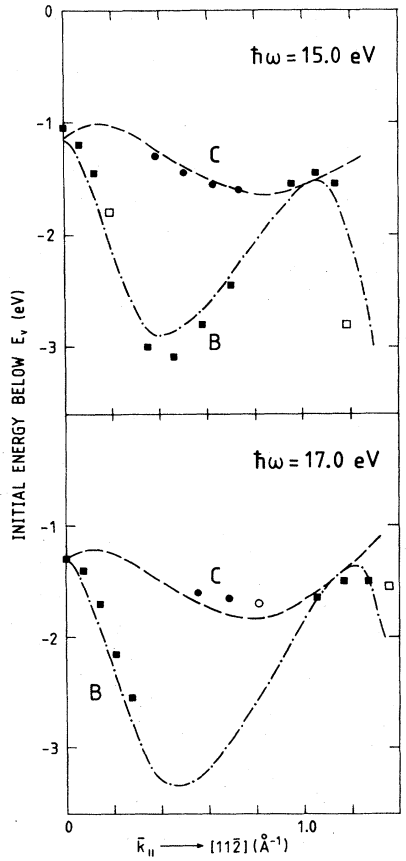

FIG. 9. Experimental and calculated $E_i(\bar{k}_{||})$ dispersions for structures B and C for $\hbar\omega = 15.0$ and 17.0 eV. For details see Fig. 5.

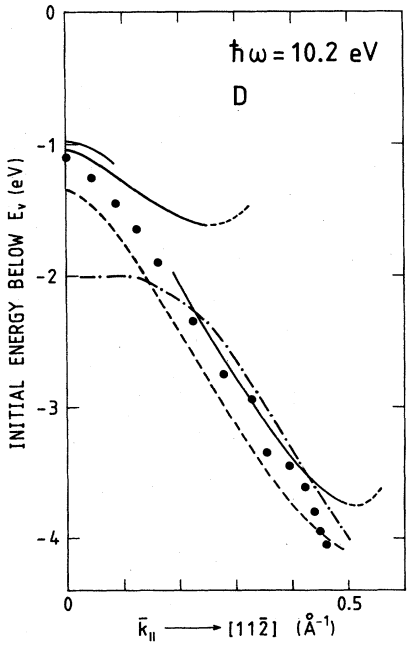

FIG. 10. Experimental $E_i(\bar{k}_{||})$ dispersion for structure D (solid circles). Calculated dispersions for different direct transitions are included. The different dispersion curves correspond to transitions from VB 2 to the $\bar{k}+\bar{G}_{111}$ final band (dashed-dotted line), from VB 3 to the $\bar{k}+\bar{G}_{\bar{1}11}$, $\bar{G}_{1\bar{1}1}$ final band (dashed line) and finally from VB 3 to three different calculated final bands (solid lines).

As can be seen from Fig. 2 there are calculated bands which closely resemble the $\overline{G}_{\bar{1}\bar{1}1,\bar{1}11}$ free-electron bands along Γ—L. From this we can expect that the use of calculated bands would also give dispersions in reasonable agreement with experiment for structure D. To account for the entire dispersion observed experimentally, we have to involve three different final bands. Only even parity bands need be considered, resulting in three different branches shown by the solid lines in Fig. 10. The even parity VB 3 serves as initial band for all branches. The changes in emission intensity could be an effect of the different final bands involved. The region of high emission intensity corresponds to transitions from VB 3 to conduction band (CB) 8.

At a photon energy of 13.0 eV, the use of free-electron final bands predicts dispersions of the similar shape as for 10.2 eV, but shifted to lower initial energies. In the 13.0-eV spectra for the $\overline{A}_{||}$ case (Fig. 6), a structure is observed at -3.5 eV for $\theta_e = 15°$ (E), which disperses downwards, crossing the energy position of the stationary -4.7-eV peak. In this limited $\overline{k}_{||}$ range, the dispersion agrees well with that obtained using the two types of free-electron bands in the region where the calculated dispersion curves come close to each other.

Turning to the case of calculated final bands, CB 8 is no longer a possible final band, which could explain why we do not see any structure having high emission intensity for 13.0 eV. Thus, to explain structure E with transitions to the calculated final-state bands, its origin must be different from that of structure D, while with the use of the free-electron final band it was possible to explain both D and E as transitions between the same pair of bands.

B. Si(111)2×1: [$\bar{1}\bar{1}$2] azimuth

In the [$\bar{1}\bar{1}$2]-azimuthal direction direct transitions from VB's 3 and 4 to the $\overline{G}_{111}$ free-electron band give $E_i(\overline{k}_{||})$ dispersion curves which look entirely different from those obtained from the [1$\bar{1}$2] direction. The difference can be seen by comparing Fig. 11, where the dispersions along the [$\bar{1}\bar{1}$2] direction are shown, with Fig. 5 for the [1$\bar{1}$2] direction. The strong asymmetry predicted by the free-electron final band is also observed experimentally. The upper spectrum in Fig. 12 was obtained at $\theta_e = 57°$ in the [1$\bar{1}$2]-azimuthal direction. This spectrum shows a sharp structure at -1.35 eV corresponding to structures B and C close to the $\overline{k}_{||}$ point where they have the same initial energies. Since the spectrum was obtained with unpolarized light, we obtain contributions from both structures B and C. The dangling-bond emission is strong because $\theta_i = 45°$ was used. In the lower spectrum obtained at the same emission angle in the [$\bar{1}\bar{1}$2]-azimuthal direction the B,C structure has disappeared, we find instead a sharp peak (F) at a lower initial energy (-2.70 eV). The dispersion of this peak is plotted as solid circles in Fig. 11. It is difficult to identify structure F above a binding energy of -2 eV because there are at least two other structures in this energy region. The use of polarized light would probably reveal the entire dispersion curve as for the [1$\bar{1}$2] direction. The structures at ~ -3 eV in the [1$\bar{1}$2] spectrum and at ~ -1.4 eV in the [$\bar{1}\bar{1}$2] spectrum do not show any $E_i(\overline{k}_{||})$ dispersion and should not be confused with structures F and B,C, respectively. The theoretically expected splitting of the dispersion curves for large-$\overline{k}_{||}$ values, see Fig. 11, is also observed experimentally for $\theta_e > 65°$. There are several other structures

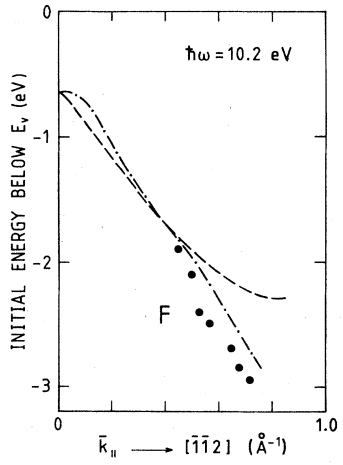

FIG. 11. Experimental $E_i(\overline{k}_{||})$ dispersion for structure F (solid circles). The calculated dispersions for direct transitions from the odd-parity and even-parity bands are included (dashed and dashed-dotted lines).

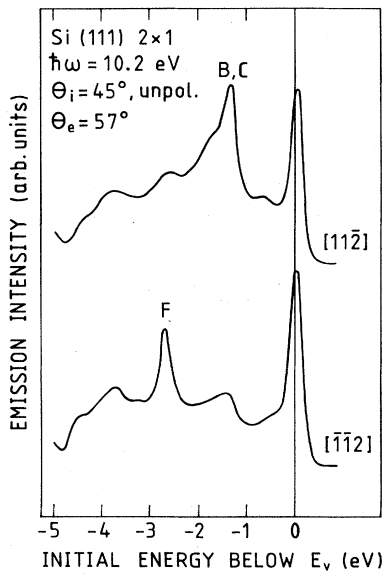

FIG. 12. Photoemission spectra obtained in the [1$\bar{1}$2] and [$\bar{1}\bar{1}$2] direction for $\theta_e = 57°$. Structure B,C corresponds to direct transitions from the two uppermost valence bands at the $\overline{k}_{||}$ point where they have the same initial energies. Structure F corresponds to direct transitions from the second-highest valence band. The spectra illustrate the asymmetry in the dispersion predicted by the $\overline{k}+\overline{G}_{111}$ free-electron band. The dangling-bond state is observed at E_v.

in the spectra which are difficult to resolve and characterize fully, since unpolarized light was used, and we will therefore leave them without an attempt to explain their origin.

C. Si(111)7×7

In this section we will discuss the differences and similarities in the bulk and surface electronic structures of Si(111)2×1 and Si(111)7×7 surfaces. The Si(111)7×7 surface was obtained in two different ways. Single-crystal Si(111) wafers of p type ($\rho \sim 5000\ \Omega$ cm) were cleaned *in situ* by Ar^+ sputtering (1000 V, 10 μA). After repeated cycles of sputtering the samples were annealed for 5 min at a temperature of 850°C. This treatment gave a sharp 7×7 low-energy electron diffraction (LEED) pattern. The Si(111)7×7 surface was also obtained by annealing the cleaved Si(111)2×1 crystal at 500°C for 10 min, which also gave a good 7×7 LEED pattern. Normal emission spectra from 7×7 and 2×1 surfaces measured at a photon energy of 10.2 eV for unpolarized light incident at an angle of 45° are compared in Fig. 13. The differences in the spectra are almost entirely limited to the dangling-bond peak. In the spectrum for the 2×1 surface, the dangling-bond peak is found at ~0.7 eV (S) below the valence-band maximum (VBM), and has a high emission intensity. After converting to the 7×7 reconstruction, we observe a dramatic decrease in emission intensity and a change in initial energy to ~0.25 eV (S_2) below the VBM for the surface-state structure.

Superimposed on the dangling-bond peak for the 2×1 surface, there should also be some contribution from the bulk peak B at ~0.6 eV below the VBM, although the contribution is expected to be small since unpolarized light at 45° incidence angle was used. For the lower-lying structures, which we interpret as being due to bulk emission, the effect of the change of surface reconstruction is small. There is an increase in emission above the VBM from an additional surface state (S_1) reaching to the Fermi level. Emission from the extra surface state was stronger for the 7×7 surface obtained by sputtering and annealing.

The 2×1 to 7×7 conversion is also followed by changes in work-function (Φ) and Fermi-level pinning. From the width of the normal emission spectra, we obtain $\Phi_{2\times1}=4.80\pm0.05$ eV and $\Phi_{7\times7}=4.60\pm0.05$ eV. The absolve values and the change in work function are consistent with values reported by other authors.[15,16] The change in Fermi-level position was obtained by aligning the bulk structure A in the two spectra. This gives

$$(E_F-E_V)_{7\times7}-(E_F-E_V)_{2\times1}=0.23\pm0.05 \text{ eV}$$

for this sample. In Fig. 14 we show spectra measured for $\theta_e=20°-30°$ along the $[1\bar{1}2]$-azimuthal direction. The lower part of the figure shows spectra for Si(111)7×7 obtained from the 2×1 reconstruction, and the upper part shows spectra for the 7×7 surface obtained from a sputtered and annealed sample. In this interval of emission angles, the two surface states (S_1 and S_2) have high emission intensities. The surface-state peaks are more pronounced for the sputtered and annealed surface. We have not detected any dispersion for these surface-state peaks along any of the $[1\bar{1}2]$-, $[\bar{1}\,\bar{1}\,2]$-, or $[1\bar{1}0]$-azimuthal directions for the 7×7 surfaces obtained in these two different ways. For the 7×7 surface there is a third surface state

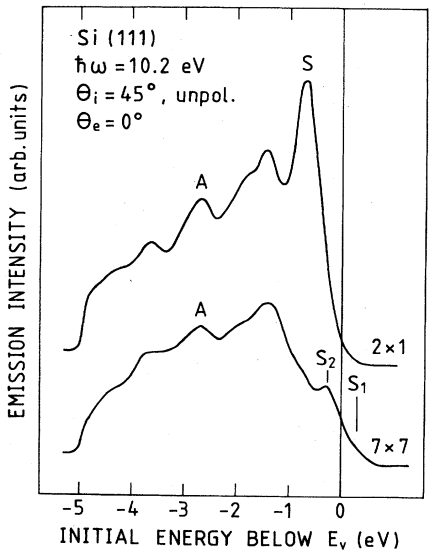

FIG. 13. Normal emission spectra for Si(111)2×1 and after converting the surface to the 7×7 reconstruction. The spectra show the different surface-state contributions.

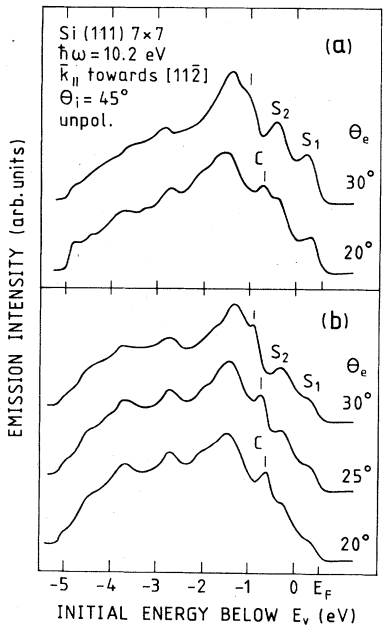

FIG. 14. Photoemission spectra for Si(111)7×7. The spectra in (a) were obtained from a sputtered and annealed sample and in (b) from a 7×7 surface obtained by annealing a Si(111)2×1 crystal.

at ~ -1.3 eV observed at higher photon energies[17] which we cannot detect at 10.2 eV because of the interference of a bulk structure at this initial energy. This surface state shows dispersion,[18,19] in contrast to S_1 and S_2, with a bandwidth of ~ 0.3 eV.[19] For off-normal emission the Si(111)2×1 surface-state emission looks entirely different from that of Si(111)7×7. Instead of two nondispersive surface-state structures near the VBM there is a highly-dispersive, high-intensity structure on the Si(111)2×1 surface (S). From the energy position of ~ -0.7 eV at $\theta_e = 0°$ (see Fig. 12) it disperses upwards along the $[1\bar{1}0]$ ($\bar{\Gamma}$–$\bar{J}$) and $[11\bar{2}]$, $[\bar{1}\,\bar{1}\,2]$ ($\bar{\Gamma}$–$\bar{K}$) directions. The total bandwidth is approximately 0.8 eV. The emission from the dangling-bond state on Si(111)2×1 has been reported elsewhere.[20,21]

In Fig. 14 there is also a dispersive structure, denoted C, not earlier reported for the 7×7 surface, which corresponds to structure C for Si(111)2×1. It is easiest to detect it in this θ_e range, where it also has the highest emission intensity observed for the 2×1 surface, although compared with the 2×1 case the intensity is drastically reduced for the 7×7 surface. A possible explanation of this observation is the increase in surface scattering introduced by the many 7×7 reciprocal-lattice vectors. The experimental dispersion of structure C for 7×7 is plotted as solid circles in Fig. 15 together with the dispersion for Si(111)2×1 (open circles). The calculated dispersion for the direct transition between VB 4 and the $\bar{G}_{111}$ free-electron band is also shown in the figure.

We find that the dispersions of C for Si(111)2×1 and Si(111)7×7 are identical within the experimental uncertainty. The comparison above shows that we can identify direct transitions from the odd parity valence band (VB 4) to the free-electron-like final band also in the spectra from Si(111)7×7. The direct transitions from the even parity valence band (VB 3), structure B in Fig. 3, are not possible to identify for 7×7 because of its lower emission intensity and the presence of other structures in that initial-energy region.

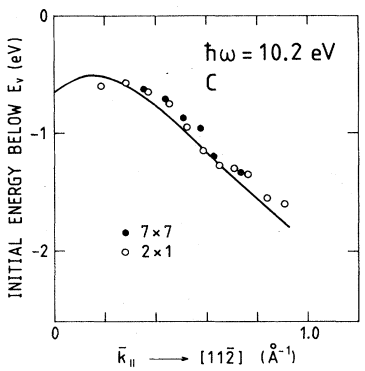

FIG. 15. Experimental $E_i(\bar{k}_{||})$ dispersions for structure C obtained from Si(111)7×7 (solid circles) and Si(111)2×1 (open circles). The solid line corresponds to the calculated dispersion for direct transitions from VB 4 to the $\bar{k}+\bar{G}_{111}$ final band.

The direct transition structures D and F observed in the $[11\bar{2}]$ and $[\bar{1}\,\bar{1}\,2]$ directions, respectively, for the 2×1 surface can only be seen as very weak structures at certain emission angles. It is not possible to obtain any $E_i(\bar{k}_{||})$ dispersion relations for these structures. The use of polarized light would probably reveal the dispersion for structures B, D, and F on the 7×7 surface as well.

IV. DISCUSSION

We have shown that three dominating structures (B, C, and F) in the photoemission spectra from Si(111) surfaces are due to direct transitions from the uppermost two valence bands to a free-electron-like final band, which can be approximated by the $\bar{k}+\bar{G}_{111}$ free-electron band. The structures were observed for a wide range of photon energies and emission angles in the $(1\bar{1}0)$-mirror plane. The identifications were made possible because of the strong polarization dependence shown by structures B and C.

The simple free-electron final band gives calculated $E_i(\bar{k}_{||})$ dispersions in surprisingly good agreement with experiment for the photon-energy range 10.2–17.0 eV investigated. In another experiment at $\hbar\omega = 21.2$ eV on Si(111)7×7 and Si(111)$\sqrt{3}\times\sqrt{3}$:Al,[19] the direct transitions from the uppermost two valence bands were also observed. The experimental dispersions are well reproduced by the calculated dispersions also for this higher photon energy.

The application of a free-electron final-state band for silicon, which has a calculated band structure deviating substantially from one that can be considered as "free-electron-like," might at first seem questionable. However, along the Γ–K like in Fig. 2 there are two parts of the calculated conduction bands, at ~ 2 eV below the steep $\bar{k}+\bar{G}_{111}$ band that have dispersions in close agreement with the free-electron band. Such calculated final bands can explain a free-electron-like behavior of the final band in photoemission. Also in the Γ–L direction there are parts of calculated conducting bands (Λ_1) that can possibly explain an apparent free-electron behavior of the final band, although the hybridization gaps are larger in this direction. We did not observe any effect of these gaps, such as a decrease in emission intensity. A normal emission experiment with smaller photon-energy steps would reveal any effects of these band gaps.

The $\bar{k}+\bar{G}_{111}$ free-electron band has certainly been proved to be useful when interpreting spectral features as being due to direct bulk transitions, like B, C, and F. When the origins of these structures now are known, we think it would be fruitful to perform more extensive photoemission studies to reveal the details of the conduction-band structure.

The 2×1 and 7×7 reconstructions of the Si(111) surface exhibit very different surface electronic structures. The highly dispersive dangling-bond band on Si(111)2×1 is replaced by three surface states on the 7×7 surface. As discussed elsewhere,[19] we find that all three surface states are probably associated with dangling-bond electrons, which is in contrast to an earlier Λ_3 symmetry assignment of the S_3 surface state.[17] The results presented here for

the surface states are in good agreement with those obtained in earlier studies for Si(111)2×1 (Refs. 20 and 21) and Si(111)7×7 (Ref. 19).

ACKNOWLEDGMENTS

This work was supported by the Swedish Natural Science Research Council.

[1]Y. Petroff and P. Thiry, Appl. Opt. **19**, 3957 (1980).
[2]F. J. Himpsel, Appl. Opt. **19**, 3964 (1980).
[3]T.-C. Chiang, J. A. Knapp, M. Aono, and D. E. Eastman, Phys. Rev. B **21**, 3513 (1980).
[4]J. G. Nelson, W. J. Gignac, R. S. Williams, S. W. Robey, J. G. Tobin, and D. A. Shirley, Surf. Sci. **131**, 290 (1983).
[5]R. D. Bringans and H. Höchst, Phys. Rev. B **25**, 1081 (1982).
[6]J. E. Rowe, M. M. Traum, and N. V. Smith, Phys. Rev. Lett. **33**, 1333 (1974); M. M. Traum, J. E. Rowe, and N. V. Smith, J. Vac. Sci. Technol. **12**, 298 (1975).
[7]C. A. Feldman, R. Engelhardt, T. Permien, E. E. Koch, and V. Saile, Nucl. Instrum. Methods **208**, 785 (1983).
[8]F. J. Himpsel, Th. Fauster, and G. Hollinger, Surf. Sci. **132**, 22 (1983).
[9]P. E. S. Persson (unpublished).
[10]C. S. Wang and B. M. Klein, Phys. Rev. B **24**, 3393 (1981), and references therein.
[11]F. J. Himpsel, P. Heiman, and D. E. Eastman, Phys. Rev. B **24**, 2003 (1981).
[12]J. Hermansson, Solid State Commun. **22**, 9 (1977).
[13]R. I. G. Uhrberg, G. V. Hansson, U. O. Karlsson, J. M. Nicholls, P. E. S. Persson, S. A. Flodström, R. Engelhardt, and E. E. Koch, Phys. Rev. Lett. **52**, 2265 (1984).
[14]G. V. Hansson, R. I. G. Uhrberg, and J. M. Nicholls, Surf. Sci. **132**, 31 (1983).
[15]G. M. Guichar, M. Balkanski, and C. A. Sébenne, Surf. Sci. **86**, 874 (1979).
[16]W. Mönch, Surf. Sci. **63**, 79 (1977).
[17]D. E. Eastman, F. J. Himpsel, J. A. Knapp, and K. C. Pandey, in *Proceedings of the 14th International Conference on the Semiconductors, 1978,* edited by B. H. Wilson (IOP, London, 1979), p. 1059.
[18]H. Neddermeyer, U. Misse, and P. Rupieper, Surf. Sci. **117**, 405 (1982).
[19]R. I. G. Uhrberg, G. V. Hansson, J. M. Nicholls, P. E. S. Persson, and S. A. Flodström, following paper [Phys. Rev. B **34**, 3805 (1985)].
[20]R. I. G. Uhrberg, G. V. Hansson, J. M. Nicholls, S. A. Flodström, Surf. Sci. **117**, 394 (1982).
[21]R. I. G. Uhrberg, G. V. Hansson, J. M. Nicholls, S. A. Flodström, Phys. Rev. Lett. **48**, 1032 (1982).